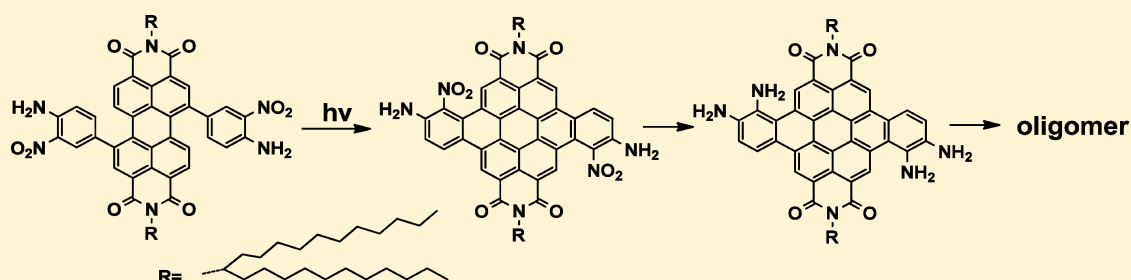


## Regioselective Photocyclization To Prepare Multifunctional Blocks for Ladder-Conjugated Materials

Zhenbo Zhao, Youdi Zhang, and Yi Xiao\*

State Key Laboratory of Fine Chemicals, Dalian University of Technology, 2 Linggong Road, Dalian 116024, China

**S** *Supporting Information*



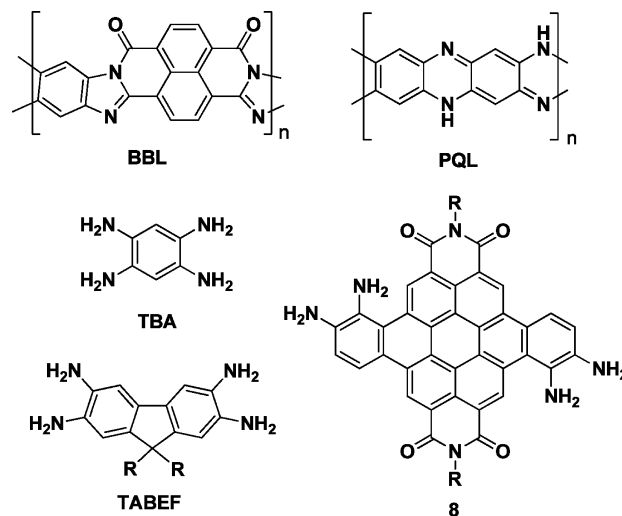
**ABSTRACT:** Multifunctional building blocks **8** and **9** were efficiently synthesized by fusing a perylene-3,4,9,10-tetracarboxylic acid bisimide (PBI) core with *o*-phenylenediamine, and they were condensed with a pyrenedione and a pyrenetetraone, respectively, to construct new ladder-type conjugated oligomers **12** and **13**. In the key photocyclization step, an unusual regioselectivity at the position ortho to the nitro group was discovered in the coupling of the *o*-nitroaniline functional units at the bay sites of PBI. Bulk-heterojunction solar cells based on **12** and **13** as the acceptors exhibited reasonable performance.

## ■ INTRODUCTION

Ladder-conjugated oligomers or polymers, because of their potential applications in electronics and optoelectronics, such as organic light-emitting diodes (OLEDs), organic thin-film transistors (OTFTs), organic photovoltaic cells, and organic solid lasers, have attracted much interest. For example, with a mobility that rivals that of amorphous Si<sup>1</sup> and reasonable air stability,<sup>2</sup> pentacene and its derivatives are a common choice for the transport layer in TFTs;<sup>3</sup> **BBL** with a planar ladder-conjugated system (Chart 1) shows high performance in air-stable organic field-effect transistors and solar cells;<sup>4</sup> and **LPPP** and its derivatives with ladder-conjugated systems have been utilized in efficient solution-processable blue LEDs.<sup>5</sup> Their rigid and planar frameworks not only facilitate electron delocalization and enhance the conductivity but also exhibit high resistance to mechanical, thermal, and chemical degradation.<sup>6</sup>

Among all the basic factors, multifunctional building blocks are essential for designing and synthesizing ladder-conjugated oligomers or polymers. For example 1,2,4,5-tetraaminobenzene (**TBA**) (Chart 1), as the key building block of **BBL**-like heteroaromatic ladder polymers, contributes to such outstanding electronic and optical properties. However, **TBA** lacks solubility-improving substituents, which makes **BBL** and its analogue polymer **PQL** (Chart 1) insoluble in a variety of organic solvents and causes processing difficulties in device fabrication. Poor solubility not only inhibits some characterizations and material processing but also causes some structure defects such as deterioration in the thermal, physical, and electrochemical properties.<sup>7</sup> 2,3,6,7-Tetraamino-9,9-bis(2-ethylhexyl)fluorene (**TABEF**) (Chart 1), as an alternative to **TBA**, readily undergoes a condensation reaction with

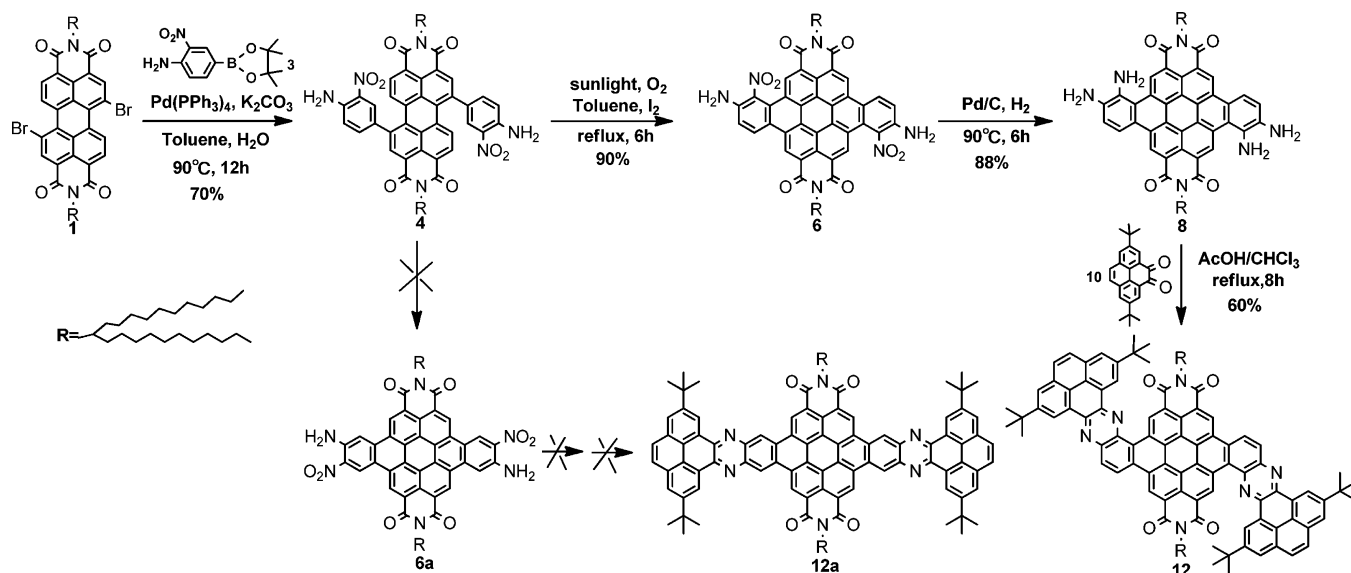
**Chart 1. Structures of the Ladder-Conjugated Polymers BBL and PQL, the Known Multifunctional Monomers TBA and TABEF, and the New Building Block 8 Designed in This Work**



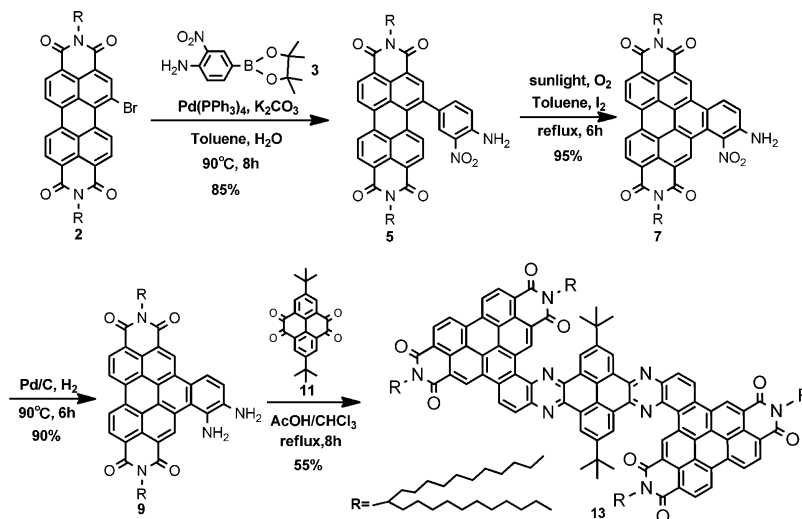
dicarboxylic acid substrates to give corresponding ladder-type model compounds with good solubility.<sup>8</sup> However, the small, planar, electron-rich fluorenyl moiety is not the most ideal unit for building n-type ladder-conjugated oligomers or polymers. Thus, the design and synthesis of novel multifunctional

Received: March 29, 2013

Scheme 1. Synthetic Route to Ladder-Conjugated Oligomer 12



Scheme 2. Synthetic Route to Ladder-Conjugated Oligomer 13



building blocks by introducing functional units, such as tetraamino and diamino groups, is a significant and ongoing challenge for building ladder-conjugated oligomers or polymers.

## RESULTS AND DISCUSSION

**Regioselectivity of Photocyclization and Synthesis.** In our strategy, we designed and synthesized the two multifunctional building blocks tetraamine 8 (Scheme 1) and diamine 9 (Scheme 2) for use in constructing novel ladder-conjugated oligomers 12 and 13, respectively. A perylene-3,4,9,10-tetracarboxylic acid bisimide (PBI) unit, as a promising building block, was introduced. First, the electronegativity of PBI can enhance the stability of oligomers, and second, it also has a significant impact on the electron distribution and the capability of self-assembly into ordered supramolecular structures.<sup>9–13</sup> In addition, swallowtail chains and *tert*-butyl groups were attached onto the peripheries to ensure good solubility and suppress molecular aggregation.

In our syntheses, photocyclization of different functional units at the bay sites of the perylene unit is the key and efficient

way to obtain ring-expanded multifunctional building blocks. In our recent work, we found that sunlight-driven photocyclization at the bay sites of perylene using phenyl substituents can lead two regioisomers,<sup>14</sup> while employing monosubstituted functional units such as thienyl, carbazolyl, thieno[3,2-*b*]thiophenyl, monosubstituted phenyl, and Schiff base, affords only one regioisomer.<sup>14,15</sup> The regioselectivity of photocyclization reactions, especially for photocyclization with disubstituted functional units, have rarely been mentioned in previous work. That will be a big obstacle in the further utilization of this approach for building multifunctional blocks and constructing ladder-conjugated oligomers and polymers. Thus, it is instructive to study the photocyclization regioselectivity at the bay sites of perylene to obtain planar ladder-conjugated oligomers.

However, in our key photocyclization step, an unusual regioselectivity was discovered. As shown in Figure 1, for two substituents X and Y (corresponding to the NO<sub>2</sub> and NH<sub>2</sub> substituents, respectively, in compound 4 in Scheme 1 and compound 5 in Scheme 2), photocyclization at the bay sites of perylene theoretically could occur at either the ortho position

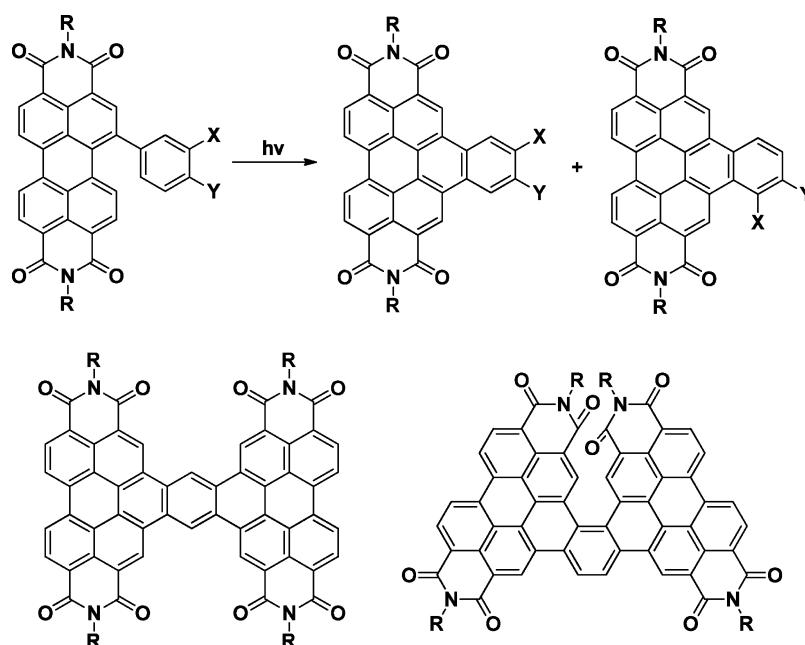


**Figure 1.** Illustrations of regioselective photocyclization and structures of disubstituted phenyl regioisomeric oligomers.

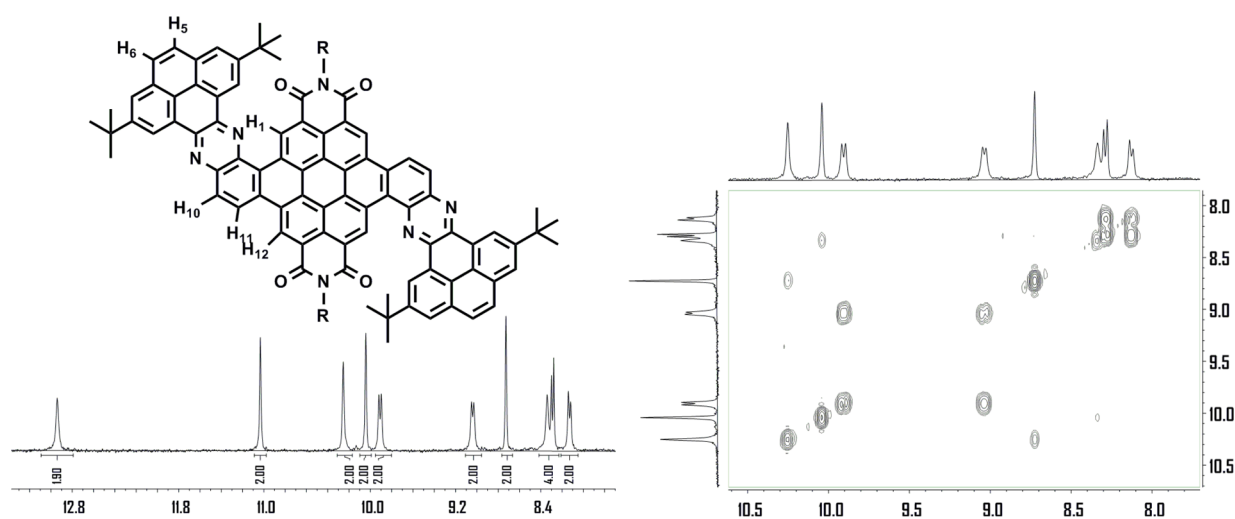


**Figure 2.** Expanded aromatic regions of the <sup>1</sup>H NMR and gCOSY spectra of compound 12 in 1,2-dichlorobenzene-*d*<sub>4</sub>.

or the para position relative to substituent X, generating two regioisomers. In view of the steric effect, photocyclization should be more likely to occur at the position para to X. However, as shown in Scheme 1, we found that photocyclization happened only at the position ortho to the nitro group. This phenomenon has not been discovered previously.

Suzuki coupling reactions were adopted to link perylene units 1 and 2 with 2-nitroaniline boronic ester 3 by single bonds, giving 4 (70%; Scheme 1) and 5 (85%; Scheme 2), respectively. Next, photocyclization was carried out to accomplish the fusion to form the corresponding ladder-conjugated intermediates 6 (90%) and 7 (95%). Hydrogenations using H<sub>2</sub> over Pd/C afforded the tetraamine and diamine intermediates 8 and 9, respectively. Following typical condensation–coupling reactions between 1,2-diamines and 1,2-diketones,<sup>16</sup> twofold condensations of 8 with 10 and 9 with 11 were carried out, during which excess diketone 10 and diamine 9 were necessary to ensure completion of the multiple condensation reactions.

The chemical structures of the targeted oligomers 12 and 13 were unambiguously characterized by NMR spectroscopy and MALDI-TOF mass spectrometry. In our synthetic strategy to obtain oligomers 12 and 13, the ring expansion is one key. Theoretically, photocyclization of compound 4 should generate two regioisomers, 6 and 6a, but only one dominant product, 6 (yield over 90%), was found. Although this photocyclization product has very good solubility in chloroform and dichloromethane, poor signals were still observed in the aromatic region of the NMR spectra, especially in the <sup>13</sup>C NMR spectra. Such a phenomenon can be attributed to the strong aggregation effect of the rigid core molecules in solution. Fortunately, the subsequent two steps (hydrogenation and condensation) also gave single products in high yields, and the final product showed good resolution in the <sup>1</sup>H NMR and gCOSY spectra (Figure 2). In the <sup>1</sup>H NMR spectrum, two singlet signals were observed at the lowest field. The chemical shifts of the two singlet signals at low field were 12.94 and 11.03 ppm. We assign these singlet resonances to protons H<sub>1</sub> and H<sub>12</sub>, respectively.

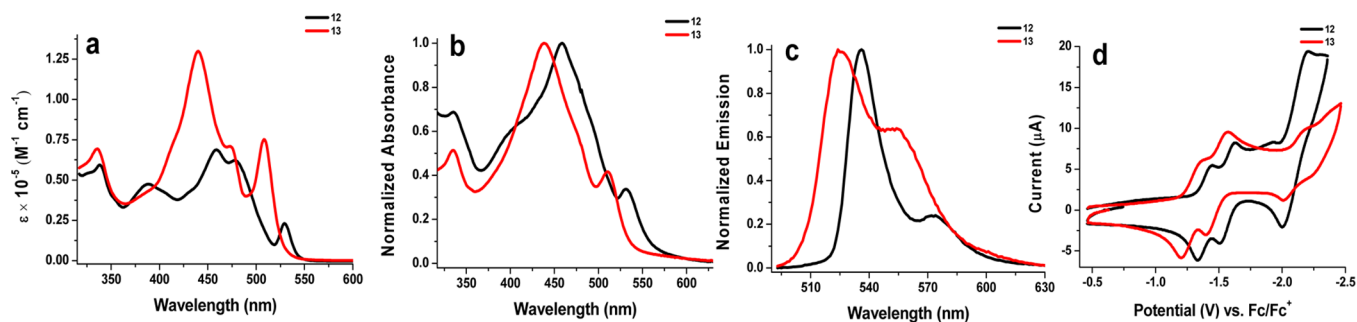


**Figure 3.** (a) UV-vis absorption spectra of **12** and **13** in chloroform solution at  $1 \times 10^{-5}$  M. (b) Normalized UV-vis absorption spectra of **12** and **13** in thin films. (c) Fluorescence spectra of **12** and **13** in chloroform. (d) Electrochemical characterization of **12** and **13** in DCM containing 0.1 M TBAPF<sub>6</sub>. The scan speed was 100 mV/s, and ferrocene/ferrocenium (Fc/Fc<sup>+</sup>) was used as an external reference.

**Table 1. Optical and Electrochemical Data for 12 and 13**

oligomer	$\lambda_{\text{abs}}^{\text{soln}}$ (nm) [ $\epsilon$ ( $\text{M}^{-1} \text{cm}^{-1}$ )]	$\lambda_{\text{abs}}^{\text{film}}$ (nm)	$E_{\text{g}}^{\text{opt}}$ (eV) <sup>a</sup>	$E_{\text{red1}}^{\circ}$ (V vs Fc/Fc <sup>+</sup> )	$E_{\text{LUMO}}$ (eV) <sup>b</sup>	$E_{\text{HOMO}}$ (eV)
<b>12</b>	458 [69 200]	464	2.19	−1.37	−3.71	−5.90
<b>13</b>	440 [130 400]	445	2.27	−1.29	−3.79	−6.06

<sup>a</sup>Optical band gap energies determined from thin films.<sup>18</sup> <sup>b</sup>Based on the assumption that the energy of Fc/Fc<sup>+</sup> is 5.08 eV relative to vacuum.<sup>18</sup>

We also found four doublet signals in the aromatic regions of oligomer **12**, and all of the *J* values were 8 Hz. The gCOSY spectrum suggested that these are two-group coupling signals that should be assigned to protons H<sub>5</sub> and H<sub>6</sub> and protons H<sub>10</sub> and H<sub>11</sub>. This evidence clearly indicates that the final product was compound **12** and not its regioisomer **12a**. Thus, we can infer that the photocyclization reaction occurred at the position ortho to the nitro group and that the product of photocyclization was **6** and not its regioisomer **6a**.

By cyclizing the 2-nitroaniliny substituents at the bay sites of the PBI core, we found an unusual regioselectivity of the photocyclization compared with that in previous work. The strong electron-withdrawing effect of the nitro group activates the ortho H more than the para H and thus favors the dehydrogenation ring closure at the ortho site. To our knowledge, most of the functional blocks that have been introduced by photocyclization at the bay sites of a perylene have been monosubstituted and electron-rich functional units, and the regioisomeric selectivity of this photocyclization has been rarely discovered and discussed. For example, functional blocks such as disubstituted phenyl, carbazolyl, thieno[3,2-*b*]thiophenyl, truxenyl, and Schiff base have been introduced by our group,<sup>14,15</sup> and monosubstituted phenyl units were introduced by Li, Zhu, and co-workers.<sup>15e,f</sup> Thienyl groups were introduced by Ko and co-workers<sup>15g</sup> and Duan and Zhan,<sup>15h</sup> and a 1,8-dicarboxymethylnaphthalene unit was introduced by Bock and co-workers.<sup>15i</sup> However, in order to obtain multifunctional blocks, it is important to understand the regioselectivity of the photocyclization resulting from the introduction of functional units containing electron-deficient or electron-rich groups. Thus, this finding is of guiding significance for future regioselective photocyclization and the introduction of multifunctional units at the bay sites of the PBI core.

**Physical Characterization.** The absorption and photoluminescence (PL) spectra of oligomers **12** and **13** in chloroform solution ( $1 \times 10^{-5}$  mol/L) and in thin films are shown in Figure 3, and the data are listed in Table 1. In solution (Figure 3a), oligomer **13** possessing two PBI segments shows a strong absorption bands across a broad range from 300 to 550 nm. There are three well-defined absorption peaks at 336, 440, and 508 nm ( $\epsilon = 69\,400$ ,  $130\,400$ , and  $76\,300 \text{ M}^{-1}$

$\text{cm}^{-1}$ , respectively). Oligomer **12** containing only one PBI segment also displays strong absorption over a broad range from 300 to 550 nm, but its maximum extinction coefficient ( $\epsilon_{\text{max}} = 69\,200 \text{ M}^{-1} \text{cm}^{-1}$ ) is considerably smaller than that of **13**. The emission peak of **12** located at 535 nm is red-shifted by 10 nm relative to the corresponding peak for **13** (Figure 3c). The quantum yields of **12** and **13** in chloroform are 0.17 and 0.15 respectively (with Rhodamine 6G as reference).<sup>17</sup> In thin films (Figure 3b), the absorption spectra of **12** and **13** become slightly broader and show red shifts compared with those in solution. Broad absorption and high extinction coefficients make **12** and **13** potential materials for solar cells and photodetectors.

The electrochemical properties of **12** and **13** were studied by cyclic voltammetry (CV) and differential pulse voltammetry (DPV) (see the Supporting Information) in DCM solution. Their reduction potentials and the calculated LUMO energies are shown in Table 1. As shown in Figure 3d, electrochemically reversible reduction waves are observed for **12** and **13**. The half-wave potentials ( $E_{\text{red1}}^{\circ}$ ) of oligomers **12** and **13** are −1.37 and −1.29 V vs Fc/Fc<sup>+</sup>, respectively. Oligomer **12** shows three reduction peaks and **13** shows four reduction peaks, implying their ability to accept at least three and four electrons, respectively. No obvious redox waves were observed upon oxidation up to 1.5 V. The LUMO energies (electron affinity) derived from the half-wave potentials are −3.71 and −3.79 eV respectively. The optical band gap energies ( $E_{\text{g}}^{\text{opt}}$ ) derived from the low-energy absorption edges in thin films are 2.19 and 2.27 eV, respectively, from which the HOMO energies were estimated as  $E_{\text{HOMO}} = E_{\text{LUMO}} - E_{\text{g}}^{\text{opt}}$ . These data indicate that oligomers **12** and **13** are potential n-type materials.

The decomposition temperatures ( $T_{\text{d}}$ , corresponding to 5% weight loss) of **12** and **13** under nitrogen are 232.7 and 389.5 °C, respectively (see the Supporting Information). The  $T_{\text{d}}$  values for **12** and **13** indicate the upper temperature limits of thermal annealing during processing. The difference in the  $T_{\text{d}}$  values for **12** and **13** may be attributed to the fact that **13** has more PBI units, which can increase the thermal stability.

**Solar Cell J–V Characterization.** Bulk heterojunction (BHJ) solar cells using poly(3-hexylthiophene) (P3HT) as the donor and oligomers **12** and **13** and their parent compound



*N,N'*-bis(12-undecyldodecyl)perylene-3,4,9,10-bis-(dicarboximide) (**PBI-C23**) as the acceptors were investigated in a preliminary study. The current density–voltage (*J*–*V*) characteristics of the BHJ solar cells are shown in Figure S3 in the Supporting Information, and the corresponding solar cell data are summarized in Table S1 in the Supporting Information. The power conversion efficiencies (PCEs) of solar cells constructed from oligomers **12** and **13** were 0.13% and 0.06%, respectively, under AM 1.5G simulated solar illumination. The moderate PCEs may result from the nonideal surface morphology of BHJ solar cell films (Figure S4 in the Supporting Information). Even so, the results for **12** and **13** are better than that for their parent compound **PBI-C23** under the same conditions.

In addition, adopting more suitable hole-transporting materials to fabricate the BHJ solar cells would be a good choice.<sup>19</sup> For example, using a lower HOMO energy polythiophene derivative with conjugated side chains (**PT1**) as the donor to fabricate BHJ solar cells with PBI-based polymers led to better film morphology and higher efficiencies than obtained using **P3HT**, as shown by the Hashimoto group.<sup>20</sup> Thus, oligomers **12** and **13** can be used as a promising n-type materials in organic solar cells.

## CONCLUSION

In summary, two multifunctional building blocks, tetraamine **8** and diamine **9**, were efficiently synthesized and used to construct novel, soluble ladder-conjugated oligomers. In the key step of photocyclization at the bay sites of **PBI**, nitro-group-induced regioisomeric selectivity has been discovered. Tetraamine **8** and diamine **9** readily underwent condensation reactions with a pyrene-4,5-dione and a pyrene-4,5,9,10-tetraone, respectively, to give the corresponding ladder-conjugated oligomers **12** and **13**. These oligomers were preliminarily applied as electron acceptors and blended with **P3HT** as the donor to fabricate BHJ solar cells, which exhibited reasonable performance.

## EXPERIMENTAL SECTION

**Materials and Characterization.** 1,7-Dibromoperylene bisimide **1**,<sup>15a</sup> 1-bromoperylene bisimide **2**,<sup>15a</sup> 2-nitro-4-(4,4,5,5-tetramethyl-1,3,2-dioxaborolan-2-yl)aniline (**3**),<sup>21</sup> pyrene-4,5-dione **10**,<sup>22</sup> and pyrene-4,5,9,10-tetraone **11**<sup>22</sup> were synthesized according to literature methods. The other reactants were purchased from commercial sources. NMR spectra were measured using TMS as an internal standard for <sup>1</sup>H and <sup>13</sup>C NMR spectroscopy. CV was performed with a standard commercial electrochemical analyzer in a three-electrode single-component cell under argon at a scan rate of 100 mV/s with a glassy carbon working electrode, a Ag/AgNO<sub>3</sub> reference electrode, a Pt disk auxiliary electrode, Bu<sub>4</sub>NPF<sub>6</sub> as the supporting electrolyte, and ferrocene (Fc) as an internal standard. Thermogravimetric analysis (TGA) was performed using dynamic scans under nitrogen. Tapping-mode atomic force microscopy (TM-AFM) was performed on an atomic force microscope. Photovoltaic devices were fabricated on indium tin oxide (ITO)-coated glass substrates with a layered structure of ITO/PEDOT:PSS/**P3HT**:**12** or **13** blend/LiF/Al. Photovoltaic performance was characterized through *J*–*V* curves recorded with a source meter under AM 1.5G illumination.

**Compound 4.** A mixture of **1** (597 mg, 0.5 mmol), **3** (291 mg, 1.1 mmol), K<sub>2</sub>CO<sub>3</sub> (744 mg, 5.5 mmol), Pd(PPh<sub>3</sub>)<sub>4</sub> (127 mg, 0.11 mmol), toluene (30 mL), H<sub>2</sub>O (2.3 mL), and EtOH (2.3 mL) was stirred at 90 °C for 12 h. Next, the crude product was purified through silica gel column chromatography with 1:1 DCM/hexane as the eluent. Compound **4** was obtained as a dark-red honeylike substance (457 mg, 70%). HRMS (MALDI-TOF MS) *m/z*: calcd for C<sub>82</sub>H<sub>110</sub>N<sub>6</sub>O<sub>8</sub>

([M]<sup>−</sup>), 1306.8385; found, 1306.8409. <sup>1</sup>H NMR (400 MHz, CDCl<sub>3</sub>): δ 0.84 (t, 12H), 1.20 (m, 72H), 1.83 (b, 4H), 2.23 (b, 4H), 5.15 (b, 2H), 6.41 (s, 4H), 6.94 (b, 2H), 7.45 (b, 2H), 7.98 (m, 2H), 8.20 (d, 1H, *J* = 8 Hz), 8.24 (d, 1H, *J* = 8 Hz), 8.6 (m, 4H). <sup>13</sup>C NMR (125 MHz, CDCl<sub>3</sub>): δ 14.3, 27.1, 29.5, 29.8, 32.0, 32.5, 54.9, 120.9, 122.1, 122.6, 122.9, 123.3, 126.8, 128.12, 129.8, 129.9, 130.2, 130.8, 131.2, 132.4, 133.0, 134.7, 135.0, 135.7, 136.8, 138.8, 139.8, 144.9, 163.6, 164.7.

**Compound 5.** A mixture of **2** (334 mg, 0.3 mmol), **3** (88 mg, 0.33 mmol), K<sub>2</sub>CO<sub>3</sub> (223 mg, 1.65 mmol), Pd(PPh<sub>3</sub>)<sub>4</sub> (38 mg, 0.033 mmol), toluene (20 mL), H<sub>2</sub>O (0.9 mL), and EtOH (0.9 mL) was stirred at 90 °C for 8 h. Next, the crude product was purified through silica gel column chromatography with 2:3 DCM/hexane as the eluent. Compound **5** was obtained as a dark-red honeylike substance (298 mg, 85%). HRMS (MALDI-TOF MS) *m/z*: calcd for C<sub>76</sub>H<sub>106</sub>N<sub>4</sub>O<sub>6</sub> ([M]<sup>−</sup>), 1170.8112; found, 1170.8149. <sup>1</sup>H NMR (400 MHz, CDCl<sub>3</sub>): δ 0.84 (t, 12H), 1.20 (m, 72H), 1.83 (b, 4H), 2.23 (b, 4H), 5.19 (m, 2H), 6.37 (s, 2H, NH<sub>2</sub>), 6.93 (d, 1H, *J* = 8 Hz), 7.37 (d, 1H, *J* = 8 Hz), 8.05 (d, 1H, *J* = 8 Hz), 8.22 (m, 1H), 8.45 (s, 1H), 8.65 (m, 5H). <sup>13</sup>C NMR (125 MHz, CDCl<sub>3</sub>): δ 14.2, 22.8, 27.0, 29.4, 29.7, 32.0, 32.5, 54.9, 120.9, 122.6, 122.9, 123.2, 123.8, 126.4, 127.7, 128.3, 128.7, 129.4, 129.6, 131.3, 132.5, 133.1, 134.5, 134.8, 135.8, 136.4, 139.2, 144.8, 163.5, 164.7.

**Compound 6.** A mixture of **4** (261 mg, 0.2 mmol), toluene (20 mL), and I<sub>2</sub> (4 mg) was illuminated with sunlight at reflux for 6 h. After distillation, the crude product was purified through silica gel column chromatography with 3:2 DCM/hexane as the eluent. Compound **6** was obtained as a red solid (234 mg, 90%). Mp: >300 °C. HRMS (MALDI-TOF MS) *m/z*: calcd for C<sub>82</sub>H<sub>106</sub>N<sub>6</sub>O<sub>8</sub> ([M]<sup>−</sup>), 1302.8072; found, 1302.8138. <sup>1</sup>H NMR (400 MHz, CDCl<sub>3</sub>): δ 0.78 (t, 12H), 1.14 (m, 54H), 1.42 (m, 18H), 2.11 (m, 4H), 2.45 (m, 4H), 5.41 (m, 2H), 6.05 (s, 4H), 7.57 (d, 2H, *J* = 8 Hz), 9.18 (s, 2H), 9.70 (d, 2H, *J* = 8 Hz), 10.15 (s, 2H). <sup>13</sup>C NMR (125 MHz, CDCl<sub>3</sub>): δ 14.2, 22.8, 27.5, 29.5, 29.8, 32.0, 32.8, 55.7, 120.9, 122.0, 122.7, 122.1, 123.9, 124.4, 124.9, 125.4, 127.1, 129.5, 131.4, 143.3.

**Compound 7.** A mixture of **5** (234 mg, 0.2 mmol), toluene (20 mL), and I<sub>2</sub> (4 mg) was illuminated with sunlight at reflux for 6 h. After distillation, the crude product was purified through silica gel column chromatography with 1:1 DCM/hexane as the eluent. Compound **7** was obtained as a red solid (222 mg, 95%). Mp: 151.9–153.4 °C. HRMS (MALDI-TOF MS) *m/z*: calcd for C<sub>76</sub>H<sub>104</sub>N<sub>4</sub>O<sub>6</sub> ([M]<sup>−</sup>), 1168.7956; found, 1168.7979. <sup>1</sup>H NMR (400 MHz, CDCl<sub>3</sub>): δ 0.87 (t, 12H), 1.17 (m, 56H), 1.39 (m, 16H), 2.01 (m, 4H), 2.33 (m, 4H), 5.26 (m, 2H), 6.20 (s, 2H), 7.54 (d, 1H, *J* = 8 Hz), 8.90 (m, 5H), 9.23 (d, 1H, *J* = 8 Hz), 9.59 (s, 1H). <sup>13</sup>C NMR (125 MHz, CDCl<sub>3</sub>): δ 14.3, 22.8, 27.4, 29.5, 29.8, 32.1, 32.6, 55.3, 121.1, 122.9, 123.0, 123.2, 123.8, 123.9, 124.2, 125.3, 125.9, 126.6, 126.9, 127.1, 127.9, 129.3, 129.6, 130.3, 131.0, 131.8, 132.8, 133.3, 143.6, 163.9, 164.9.

**Compound 8.** A mixture of **6** (261 mg, 0.2 mmol), THF (20 mL), and 10% Pd/C (30 mg) was shaken under hydrogen (5 psi) at 90 °C for 6 h, after which the reaction mixture was filtered under reduced pressure and the organics were concentrated by evaporation. In view of the unstability of the tetraamine, the resulting brown oil (218 mg, 88% yield) was used without further purification.

**Compound 9.** A mixture of **7** (234 mg, 0.2 mmol), THF (20 mL), and 10% Pd/C (26 mg) was shaken under hydrogen (5 psi) at 90 °C for 6 h, after which the reaction mixture was filtered under reduced pressure and the organics were concentrated by evaporation. In view of the unstability of the diamine, the resulting dark-red oil (205 mg, 90% yield) was used in the next step without further purification.

**Oligomer 12.** An oxygen-free mixture of CHCl<sub>3</sub> (4 mL) and acetic acid (16 mL) was added to a flask containing tetraamino compound **8** (124 mg, 0.1 mmol) and compound **10** (103 mg, 0.3 mmol) under the protection of Ar, and then the system was stirred at 135 °C overnight. After the mixture was cooled to ambient temperature, the solvent was removed under reduced pressure to give a residue. Flash silica gel column chromatography (DCM/hexane eluent) was performed to obtain the pure product **12** (112 mg, 60% yield). Mp: >300 °C (dec). HRMS (MALDI-TOF MS) *m/z*: calcd for C<sub>130</sub>H<sub>150</sub>N<sub>6</sub>O<sub>4</sub> ([M]<sup>−</sup>),

1859.1719; found, 1859.1830.  $^1\text{H}$  NMR (400 MHz,  $\text{CDCl}_3$ ):  $\delta$  0.97 (t, 12H), 1.36 (m, 20H), 1.51 (m, 20H), 1.56 (m, 8H), 1.69 (m, 8H), 1.84 (s, 18H), 1.88 (m, 8H), 2.08 (m, 8H), 2.22 (s, 18H), 2.75 (m, 4H), 3.11 (m, 4H), 6.12 (m, 2H), 8.13 (d, 2H,  $J = 8$  Hz), 8.29 (d, 2H,  $J = 8$  Hz), 8.34 (s, 2H), 8.73 (s, 2H), 9.04 (d, 2H,  $J = 8$  Hz), 9.91 (d, 2H,  $J = 8$  Hz), 10.04 (s, 2H), 10.26 (s, 2H), 11.03 (s, 2H), 12.94 (s, 2H).  $^{13}\text{C}$  NMR (125 MHz,  $\text{CDCl}_3$ ):  $\delta$  14.2, 22.8, 28.1, 29.5, 29.9, 30.3, 31.8, 32.0, 32.3, 33.3, 35.4, 36.1, 55.6, 56.2, 120.8, 121.4, 122.2, 122.4, 122.8, 123.4, 123.9, 124.3, 125.4, 126.2, 126.8, 127.3, 128.0, 128.6, 130.0, 130.6, 131.4, 140.6, 141.4, 142.2, 149.3, 150.2, 164.6, 165.0, 165.6.

**Oligomer 13.** An oxygen-free mixture of  $\text{CHCl}_3$  (4 mL) and acetic acid (16 mL) was added to a flask containing diamino compound **9** (114 mg, 0.1 mmol) and compound **11** (11 mg, 0.03 mmol) under the protection of Ar, and then the system was stirred at 135 °C overnight. After the mixture was cooled to ambient temperature, the solvent was removed under reduced pressure to give a residue. Flash silica gel column chromatography (DCM/hexane eluent) was performed to obtain the pure product **13** (43 mg, 55% yield). Mp: >300 °C. HRMS (MALDI-TOF MS)  $m/z$ : calcd for  $\text{C}_{176}\text{H}_{226}\text{N}_8\text{O}_8$  ( $[\text{M}]^-$ ), 2579.7524; found, 2579.7427.  $^1\text{H}$  NMR (400 MHz,  $\text{CDCl}_3$ ):  $\delta$  0.71 (m, 18H), 0.82 (m, 24H), 1.19 (m, 160H), 1.80 (m, 8H), 2.00 (m, 8H), 5.43 (m, 4H), 8.91 (m, 4H), 9.19–9.78 (m, 10H), 10.02 (s, 2H), 10.22 (s, 2H), 12.12 (s, 2H).  $^{13}\text{C}$  NMR (125 MHz,  $\text{CDCl}_3$ ):  $\delta$  14.1, 22.7, 27.3, 29.4, 29.7, 32.0, 32.6, 54.9, 122.8, 123.2, 124.2, 125.2, 125.9, 126.2, 126.7, 127.1, 127.2, 127.6, 129.1, 129.3, 130.1, 130.4, 131.1, 133.6, 141.4, 164.4, 165.2.

## ■ ASSOCIATED CONTENT

### ■ Supporting Information

Detailed experimental procedures and characterization data for all new compounds;  $^1\text{H}$ ,  $^{13}\text{C}$  NMR, gCOSY, and mass spectra of the products; and DPV and TGA data for **12** and **13**. This material is available free of charge via the Internet at <http://pubs.acs.org>.

## ■ AUTHOR INFORMATION

### Corresponding Author

\*Fax: +(86)411-84986252. E-mail: xiaoyi@dlut.edu.cn.

### Notes

The authors declare no competing financial interest.

## ■ ACKNOWLEDGMENTS

We thank National Natural Science Foundation of China (21174022), the National Basic Research Program of China (2013CB733702), and the Specialized Research Fund for the Doctoral Program of Higher Education (20110041110009) for financial support.

## ■ REFERENCES

- (1) Dimitrakopoulos, C. D.; Malenfant, P. R. L. *Adv. Mater.* **2002**, *14*, 99.
- (2) Facchetti, A. *Mater. Today* **2007**, *10*, 28.
- (3) (a) Murphy, A. R.; Fréchet, J. M. J. *Chem. Rev.* **2007**, *107*, 1066. (b) Anthony, J. E. *Angew. Chem., Int. Ed.* **2008**, *47*, 452.
- (4) (a) Babel, A.; Jenekhe, S. A. *J. Am. Chem. Soc.* **2003**, *125*, 13656. (b) Alam, M. M.; Jenekhe, S. A. *Chem. Mater.* **2004**, *16*, 4647.
- (5) (a) Scherf, U. *J. Mater. Chem.* **1999**, *9*, 1853. (b) Jacob, J.; Sax, S.; Piok, T.; List, E. J. W.; Grimsdale, A. C.; Müllen, K. *J. Am. Chem. Soc.* **2004**, *126*, 6987.
- (6) (a) Yu, L. P.; Chen, M.; Dalton, L. R. *Chem. Mater.* **1990**, *2*, 649. (b) Tessler, M. M. *J. Polym. Sci., Part A: Polym. Chem.* **1966**, *1*, 2521.
- (7) (a) Kim, O.-K. *J. Polym. Sci., Polym. Lett. Ed.* **1985**, *23*, 137. (b) Stille, J. K.; Freeburger, M. E. *J. Polym. Sci., Part A-1: Polym. Chem.* **1968**, *6*, 161. (c) Jenekhe, S. A.; Johnson, P. O.; Agrawal, A. K. *Polym. Mater.: Sci. Eng.* **1989**, *60*, 404.

- (8) Li, X.; Xiao, Y.; Qian, X. *Org. Lett.* **2008**, *10*, 2885.
- (9) (a) Horowitz, G.; Kouki, F.; Spearman, P.; Fichou, D.; Nogues, C.; Pan, X.; Garnier, F. *Adv. Mater.* **1996**, *8*, 242. (b) Struijk, C. W.; Sieval, A. B.; Dakhorst, J. E. J.; van Dijk, M.; Kimkes, P.; Koehorst, R. B. M.; Donker, H.; Schaafsma, T. J.; Picken, S. J.; van de Craats, A. M.; Warman, J. M.; Zuilhof, H.; Sudhölter, E. J. R. *J. Am. Chem. Soc.* **2000**, *122*, 11057. (c) Schmidt-Mende, L.; Fechtenkötter, A.; Müllen, K.; Moons, E.; Friend, R. H.; MacKenzie, J. D. *Science* **2001**, *293*, 1119. (d) Shin, W. S.; Jeong, H.-H.; Kim, M.-K.; Jin, S.-H.; Kim, M.-R.; Lee, J.-K.; Lee, J. W.; Gal, Y.-S. *J. Mater. Chem.* **2006**, *16*, 384.
- (10) (a) Jones, B. A.; Ahrens, M. J.; Yoon, M.-H.; Facchetti, A.; Marks, T. J.; Wasielewski, M. R. *Angew. Chem., Int. Ed.* **2004**, *43*, 6363. (b) Weitz, R. T.; Amsharov, K.; Zschieschang, U.; Villas, E. B.; Goswami, D. K.; Burghard, M.; Dosch, H.; Jansen, M.; Kern, K.; Klauk, H. *J. Am. Chem. Soc.* **2008**, *130*, 4637. (c) Schmidt, R.; Ling, M. M.; Oh, J. H.; Winkler, M.; Könnemann, M.; Bao, Z.; Würthner, F. *Adv. Mater.* **2007**, *19*, 3692.
- (11) Langhals, H.; Karolin, J.; Johansson, L. B.-Å. *J. Chem. Soc., Faraday Trans.* **1998**, *94*, 2919.
- (12) (a) Quante, H.; Müllen, K. *Angew. Chem., Int. Ed. Engl.* **1995**, *34*, 1323. (b) Pschirer, N. G.; Kohl, C.; Nolde, F.; Qu, J.; Müllen, K. *Angew. Chem., Int. Ed.* **2006**, *45*, 1401. (c) Holtrup, F. O.; Müller, G. R. J.; Quante, H.; De Feyter, S.; De Schryver, F. C.; Müllen, K. *Chem.—Eur. J.* **1997**, *3*, 219.
- (13) (a) Qian, H.; Wang, Z.; Yue, W.; Zhu, D. *J. Am. Chem. Soc.* **2007**, *129*, 10664. (b) Qian, H.; Negri, F.; Wang, C.; Wang, Z. *J. Am. Chem. Soc.* **2008**, *130*, 17970. (c) Yue, W.; Lv, A.; Gao, J.; Jiang, W.; Hao, L.; Li, C.; Li, Y.; Polander, L. E.; Barlow, S.; Hu, W.; Di Motta, S.; Negri, F.; Marder, S. R.; Wang, Z. *J. Am. Chem. Soc.* **2012**, *134*, 5770.
- (14) Yuan, Z.; Xiao, Y.; Qian, X. *Chem. Commun.* **2010**, *46*, 2772.
- (15) (a) Yuan, Z.; Xiao, Y.; Yang, Y.; Xiong, T. *Macromolecules* **2011**, *44*, 1788. (b) Yang, Y.; Wang, Y.; Xie, Y.; Xiong, T.; Yuan, Z.; Zhang, Y.; Qian, S.; Xiao, Y. *Chem. Commun.* **2011**, *47*, 10749. (c) Xie, Y.; Zhang, X.; Xiao, Y.; Zhang, Y.; Zhou, F.; Qu, J. *Chem. Commun.* **2012**, *48*, 4338. (d) Zhang, Y.; Zhao, Z.; Cheng, C.; Xiao, Y. *RSC Adv.* **2012**, *2*, 12644. (e) Li, Y.; Zheng, H.; Li, Y.; Wang, S.; Wu, Z.; Liu, P.; Gao, Z.; Liu, H.; Zhu, D. *J. Org. Chem.* **2007**, *72*, 2878. (f) Li, Y.; Xu, L.; Liu, T.; Yu, Y.; Liu, H.; Li, Y.; Zhu, D. *Org. Lett.* **2011**, *13*, 5692. (g) Choi, H.; Paek, S.; Song, J.; Kim, C.; Cho, N.; Ko, J. *Chem. Commun.* **2011**, *47*, 5509. (h) Zhou, W.; Jin, F.; Hung, X.; Duan, X.; Zhan, X. *Macromolecules* **2012**, *45*, 7823. (i) Kelber, J.; Achard, M. F.; Durola, F.; Bock, H. *Angew. Chem., Int. Ed.* **2012**, *51*, 5200.
- (16) Stille, J. K.; Mainen, E. L. *Macromolecules* **1968**, *1*, 36.
- (17) Fischer, M.; Georges, J. *Chem. Phys. Lett.* **1996**, *260*, 115.
- (18) Thompson, B. C.; Kim, Y. G.; McCarley, T. D. *J. Am. Chem. Soc.* **2006**, *128*, 12714.
- (19) Sharma, G. D.; Suresh, P.; Mikroyannidis, J. A.; Stylianakis, M. M. *J. Mater. Chem.* **2010**, *20*, 561.
- (20) Zhou, E.; Cong, J.; Wei, Q.; Tajima, K.; Yang, C.; Hashimoto, K. *Angew. Chem., Int. Ed.* **2011**, *50*, 2799.
- (21) Hubbard, R. D.; Bamaung, N. Y.; Fidanze, S. D.; Erickson, S. A.; Palazzo, F.; Wilsbacher, J. L.; Zhang, Q.; Tucker, L. A.; Hu, X.; Kovar, P.; Osterling, D. J.; Johnson, E. F.; Bouska, J.; Wang, J.; Davidsen, S. K.; Bell, R. L.; Sheppard, G. S. *Bioorg. Med. Chem. Lett.* **2009**, *19*, 1718.
- (22) Hu, J.; Zhang, D.; Harris, F. W. *J. Org. Chem.* **2005**, *70*, 707.